Journal of Thermal Analysis and Calorimetry, Vol. 59 (2000) 807–814

KINETIC AND THERMODYNAMIC STUDIES OF FACIAL AND MERIDIONAL *uns-cis*-[Co(eddp)gly] COMPLEXES

N. Petranović[1], *D. Minić*[1], *T. J. Sabo*[2] *and D. Doković*[2]

[1]Faculty of Physical Chemistry, University of Belgrade, P.O. Box 173, 11000 Belgrade
[2]Faculty of Chemistry, University of Belgrade, P.O. Box 158, 11000 Belgrade, Yugoslavia

(Received January 10, 1998; in revised form March 16, 1999)

Abstract

Thermal properties of facial and meridional *uns-cis*-[Co(eddp)gly]·$0.5H_2O$ complexes were investigated by means of DSC and TG techniques. It was shown that the processes of thermal decomposition of these complexes are multi-step degradation processes, which can also be well separated into individual steps, depending on the molecular symmetry. Thus, the process of thermal degradation of the meridional isomer of the above complex consists of 4 well-separated steps in the temperature interval from 100 to 500°C. The corresponding kinetic and thermodynamic parameters of this process were determined, and a possible mechanism is discussed.

Keywords: facial and meridional Co(III) complexes, kinetics, thermodynamics

Introduction

New complexes of cobalt(III) have been synthesized, with ethylenediamine-N,N'-di-3-propionate (eddp) and glycine anions as ligands [1]. Theoretically, these compounds can exist as three geometric isomers [1]. However, it can be deduced from previous work [2] that complexing with eddp favours the *uns-cis* configuration. Consequently, two geometric isomers are expected: a facial and a meridional *uns-cis*-(ethylenediamine-N,N'-3-propionato)(glycinato)cobalt(III) complex.

These compounds, and also some similar, previously described complexes, are of vital importance in studying processes in biological systems. It is recognized that they cause hyperglycemia [3], increase albumin content [4], and stimulate kerotene synthesis, while it is also noted that they stimulate growth [5]. Besides being of importance in biological systems, these compounds can be of interest from another aspect: as convenient starting substances in syntheses of novel oxide materials – nanomaterials, with ultra-fine nanoparticles. It is known [6] that for these syntheses the most favourable complexes are those that yield an oxide as a final product of thermal treatment, with elimination of other components by their gasification.

1418–2874/2000/ $ 5.00

Akadémiai Kiadó, Budapest
Kluwer Academic Publishers, Dordrecht

The objective of the present work was an investigation of the thermal decompositions of facial and meridional *uns-cis*-Co(eddp)(gly)·0.5H_2O and a thermodynamic and kinetic analysis of the accompanying processes.

Experimental

Thermal analysis

Thermal analysis was performed on a DuPont 1090 thermoanalyzer, using a DSC cell and a 951 TG thermogravimetric cell. The TG curves were obtained at a heating rate of 10°C min^{-1}, while DSC curves were obtained at different heating rates. The DSC measurements were made in H_2 atmosphere, while the TG curves were obtained in H_2 and in air.

Mass spectra

Mass spectra were recorded on a double focusing reverse geometry Finnigan-MAT 8230 mass spectrometer at resolution 1000, using a combined EI-CI source at a source temperature of 200°C. Samples were introduced by means of a DCI probe with a tungsten wire (diameter 0.08 mm). Current through the wire was programmed linearly at a rate of 40 mA s^{-1}. The technique is known as In-beam [7]. The data system used was the Finnigan INCOS SS-300, running on a DEC PDP 11/73 computer.

X-ray analysis

X-ray analysis was carried out on a Philips Analytical PW710 diffractometer, using CuK_α radiation (0.15405 nm).

Results and discussion

Thermal studies

The TG curve in an atmosphere of air (Fig. 3) shows three steps of mass loss, followed by burning at a temperature above 300°C. For this reason, the other TG curve was obtained in H_2 atmosphere.

Thermal investigation of the synthesized isomers in the temperature interval from room temperature to 550°C reveals a series of degradation stages (endothermal and exothermal, Figs 1 and 2). At 140°C, water loss takes place, after which the samples are stable until about 205°C, when stepwise degradation starts and lasts until the formation of a stable product. The X-ray powder diffraction pattern of the residue was identified as that of CoO for both isomers investigated (Powder Diffraction File No. 9-402 27).

The stepwise degradation of the facial (red) isomer proceeds with the individual steps overlapping, which prevents analysis of each step individually (Fig. 1). This be-

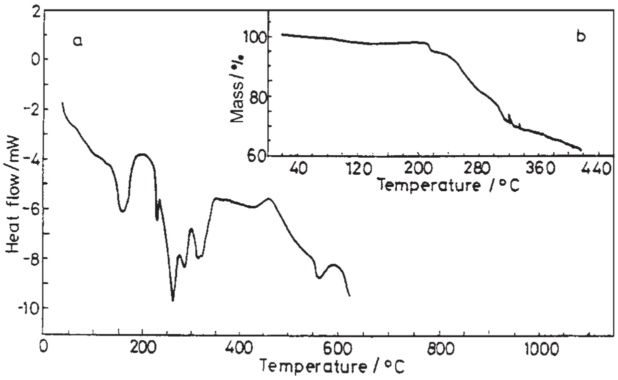

Fig. 1 DSC curves of *fac-uns-cis*-[Co(eddp)gly] in a H_2 flow; heating rate 20°C min^{-1} (a); TG curve of *fac-uns-cis*-[Co(eddp)gly] in a H_2 flow; heating rate 10°C min^{-1} (b)

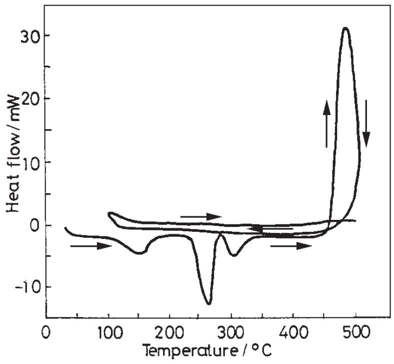

Fig. 2 DSC curves of *mer-uns-cis*-[Co(eddp)gly] for two heating cycles and one cooling cycle in a H_2 flow; heating rate 20°C min^{-1}

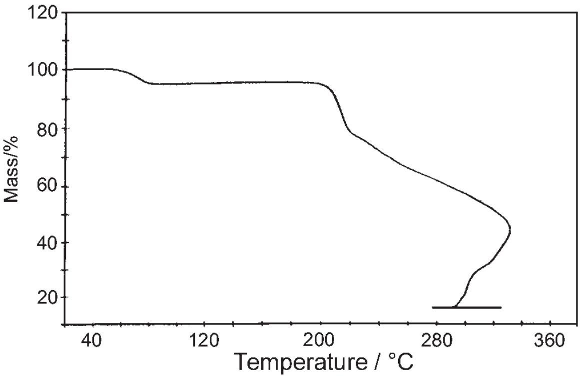

Fig. 3 TG curve of *mer-uns-cis*-[Co(eddp)gly] in an atmosphere of air; heating rate 20°C min^{-1}

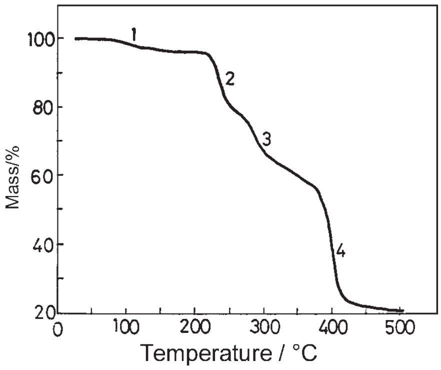

Fig. 4 TG curve of *mer-uns-cis*-[Co(eddp)gly] in a H_2 flow; heating rate 20°C min^{-1}

haviour is certainly a consequence of the structure. The structure of the red isomer is such that the beginning of degradation at 200°C causes further, almost chainwise, degradation of the remaining part of the molecule, which is manifested by overlapping of the individual degradation steps. It is therefore impossible to separate and analyze them in detail.

However, the processes of stepwise degradation in the case of the meridional (violet) isomer are well separated, which permits the determination of enthalpies (DSC, Fig. 2) and the mass losses of each of the individual steps (TG, Fig. 4, Table 1).

Table 1 TG and DSC data on *mer-uns-cis*-[Co(eddp)gly] in the temperature interval 25–600°C

TG data (a)		DSC data (b)	
T/°C	mass loss/%	T/°C	ΔH/J g^{-1}
140.5	3.98	150	92
236.8	16.91	262.7	273
283.9	15.88	301.9	101
398.6	41.90	476.3	–1753
Residue	20.7		

The DSC curve of the meridional isomer exhibits three endothermal peaks, at 150, 262.7 and 301.9°C, plus one exothermal peak, at 476.3°C (Fig. 2).

The first peak, at 150°C, is attributed to complex dehydration, which corresponds to a loss of 0.5 moles of H_2O. Two subsequent endothermal peaks, at 262.7 and 301.9°C, are well defined, but somewhat asymmetric. They are the result of changes that occur during the thermal treatment of Co(III), also evident in the corresponding TG curve (Fig. 4).

Thermal decomposition of the Co(III) complex in the atmosphere of hydrogen (Fig. 4) proceeds in four completely separate steps. The first process of mass loss of 2.98% at about 140°C, which is complementary to the first endothermal peak in the DSC curve, corresponds to a loss of 0.5 mole of crystal water. In the temperature range 140–205°C, the complex is stable, but after that thermal decomposition is observed. The results of TG curve analysis (Fig. 4) are given in Table 1a, and DSC data (Fig. 2) are given in Table 1b.

On the basis of the above results, taking into account the experimental (TG) and theoretical calculations based on mass losses, the process of thermal decomposition of the meridional isomer in the temperature range studied can be assumed to occur in the following way:

Step 1:

$$^{*}CoC_{10}H_{18}N_3O_6 \cdot 0.5H_2O \rightarrow CoC_{10}H_{18}N_3O_6 + 0.5H_2O$$

344** 335**

experimental mass loss 2.98%
calculated mass loss 2.62%

Step 2:

$$CoC_{10}H_{18}N_3O_6 \rightarrow CoC_7H_{14}N_3O_5 + CO + C_2H_4$$

335** 279**

experimental mass loss 16.91%
calculated mass loss 16.28%

Step 3:

$$CoC_7H_{14}N_3O_5 \rightarrow CoC_4H_8N_2O_5 + C_2H_4 + 0.5C_2N_2 + H_2$$

279** 223**

experimental mass loss 15.88%
calculated mass loss 16.28%

Step 4:

$$CoC_4H_8N_2O_5 \rightarrow CoO + 2H_2O + 0.5H_2 + CO_2 + N_2 + 1.5C_2H_2$$

223** 75**

experimental mass loss 41.90%
calculated mass loss 43.02%

**mer-uns-cis*-[Co(eddp)gly]·0.5H_2O=Co($C_{10}H_{18}N_3O_6$)·0.5H_2O

**relative molecular mass

Residue:

experimental mass loss 22.33%
calculated mass loss 21.80%

In the mechanism presented, Step 1 corresponds to the loss of crystal water. Step 2 is attributed to the release of C_2H_4 and CO. Exactly at 262.7°C, the coordinated glycine of the anhydrous compound begins to decompose. Free glycine actually decomposes at 232°C, and the higher temperature of glycine decomposition in the investigated complex can be attributed to the higher stability of glycine as a result of coordination. Step 3 is attributed to the release of C_2H_4, $1/2C_2N_2$ and H_2. The eddp ligand is similar to the edta ligand. Accordingly, similar decompositions of eddp and edta complexes can also be expected. Obviously, in this step the complex losses fragments of the coordinated eddp ligand. Fragment C_2H_4 is derived from the backbone diamine ring. Finally, in Step 4 the complex decomposes to CoO.

The results presented are in accordance with the results of thermal analysis of edta and its salts complexes [8]. We are inclined to attribute the exothermal peak at 476.3°C to the formation-crystallization of cobalt(II) oxide, which, according to the mechanism proposed, arises in Step 4, as the final product of the decomposition of coordinately bound ligands, which also liberates CO, H_2O, N_2 and H_2. The total enthalpy change for this process is ΔH=–1753 J g^{-1}, derived as the sum of the endothermal effects of decomposition and the exothermal effect of crystallization, which dominates the total sum.

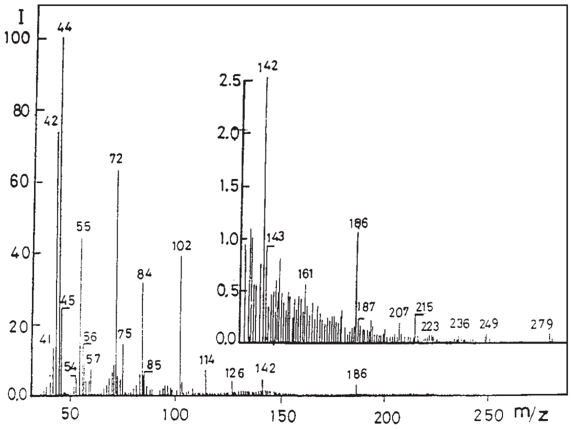

Fig. 5 Mass spectra of meridional *uns-cis*-[Co(eddp)gly]

The results of thermal analysis suggest a higher thermodynamic stability of the meridional isomer than that of the facial isomer of *uns-cis*-[Co(eddp)gly]. Also, these results suggest that the higher thermodynamic stability of the meridional isomer is the dominant factor in the distribution of the isomers (mer:fac=12:1, see experimental section).

For a more detailed analysis of these processes, a mass spectrum, presented in Fig. 5, was used. It shows the presence of all molecular species that are proposed to be formed on sample decomposition. The absence of the parent ion (m/z=335) from the mass spectrum can be explained by its fast degradation, or by thermal degradation precluding the transformation of the starting material, in the gaseous phase. Degradation of the anhydrous complex in the first phase of Step 2 gives rise to molecular species C_2H_4 and CO, along with the formation of an ion with m/z 279. The presence of ions with m/z 249, 186, 142 and 114 results from the degradation of the primary products of thermal degradation of the ion with m/z 279, according to the following reactions:

Step 3:

$CoC_7H_{14}N_3O_5 \rightarrow CoC_5H_8N_3O_5 + C_2H_4 + H_2$

m/*z*=279 *m*/*z*=249

$CoC_5H_8N_3O_5 \rightarrow CoC_4H_8N_2O_5 + 0.5C_2N_2$

m/*z*=249 *m*/*z*=223

Step 4:

$CoC_4H_8N_2O_5 \rightarrow CoC_4H_3N_2O_3 + 2H_2O + 0.5H_2$

m/*z*=223 *m*/*z*=186

$CoC_4H_3N_2O_3 \rightarrow CoC_3H_3N_2O + CO_2$

m/*z*=186 *m*/*z*=142

$CoC_3H_3N_2O \rightarrow CoC_3H_3O + N_2$

m/*z*=142 *m*/*z*=114

$CoC_3H_3O \rightarrow CoO + 1.5C_2H_2$

m/*z*=114 *m*/*z*=75

Kinetic analysis of the process

The thermal effect observed in the DSC curves are not suitable for kinetic analysis, because the peaks are complex (asymmetric and very close to one another), except for the exothermal one at 476.3°C. Comparison of the results of the DSC and TG analyses leads to the conclusion that the DSC diagram probably contains combined but overlapping thermal effects of Steps 2 and 3.

However, the TG curve in Fig. 2b displays well-separated processes, which allows a kinetic analysis of Steps 2 through 4, by applying Coats-Redfern [9] and Dobovišek-Zivković [11] methods, i.e. determining the reaction order and the activation energy of the process. The results of this analysis are presented in Table 2.

Table 2 Kinetic parameters of *mer-uns-cis*-[Co(eddp)gly] derived from TG data

Coats-Redfern method [9]				Dobovišek-Zivković method [11]		
Step	E/kJ mol^{-1}	n	R	Step	E/kJ mol^{-1}	R
2	375	1	99895	2	345	99888
3	225	1	99896	3	214	99889
4	325	1	99709	4	321	99878

The reaction order n=1 is typical for reactions of decomposition where the surface is decomposed by first-order kinetics.

In order to obtain kinetic parameters for the process that corresponds to the endothermal effect at 150°C in the DSC curve and for the exothermal process at

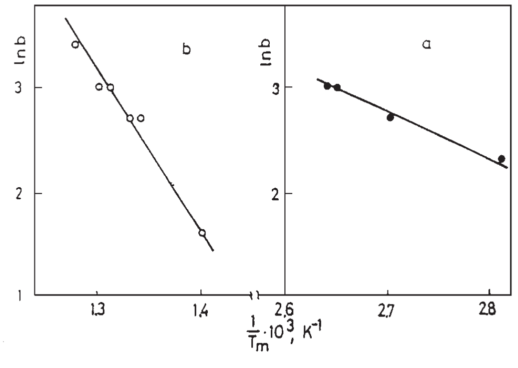

Fig. 6 Arrhenius plots of ln*b* *vs*. $1/T_m$: a – process of dehydration; b – process of crystallization of meridional *uns-cis*-[Co(eddp)gly]

476.3°C, we used the Ozawa method [10], which relates the heating rate variation, *b*, with the peak temperature T_m (Fig. 6). The plots of ln*b* *vs*. $1/T_m$ were used to determine the activation energies, found to be 411 and 130 kJ mol^{-1}, respectively.

* * *

This work was supported by the Ministry of Science of the Republic of Serbia.

References

1 T. Sabo, S. Grgurić, D. Minić and S. Trifunović, J. Coord. Chem., 44 (1998) 47.
2 D. J. Radanović, M. I. Đuran, V. D. Miletić and R. R. Parijez, J. Serb. Chem. Soc., 50 (1985) 99.
3 J. H. Koch, Nature, 175 (1955) 856.
4 H. E. Amelung, H. J. Henschel and N. Hartman, Acta Biol. Med. Ger., 13 (1964) 185.
5 V. G. Znachkova and Kh. Sh. Kazanov, Usp. Zap. Kazan. Vet. Inst., 97 (1966) 177.
6 A. S. Nikolić, Master Thesis, University of Belgrade, 1993.
7 A. Dell, D. H. Williams, H. R. Morris, G. A. Smith, J. Feney and G. C. K. Roberts, J. Am. Chem. Soc., 97 (1975) 2497.
8 W. W. Wendlandt, Anal. Chem., 33 (1960) 848.
9 A. W. Coats and J. P. Redfern, Nature, 201 (1964) 68.
10 T. Ozawa, J. Thermal Anal., 2 (1970) 301.
11 Z. Zivković and B. Dobovišek, Thermochim. Acta, 32 (1979) 205.
12 N. Petranović, U. Mioć and D. Minić, Thermochim. Acta, 116 (1987) 137.